

*JAMES*

Supporting Information for

**Forward modeling of bending angles with a two-dimensional operator for GNSS airborne radio occultations in atmospheric rivers**

P. Hordyniec<sup>1,2</sup>, J. S. Haase<sup>2</sup>, M. J. Murphy, Jr.<sup>3,4</sup>, B. Cao<sup>2</sup>, A. M. Wilson<sup>5</sup>, I. H. Banos<sup>6</sup>

<sup>1</sup>Institute of Geodesy and Geoinformatics, Wrocław University of Environmental and Life Sciences, Wrocław, Poland

<sup>2</sup>Scripps Institution of Oceanography, University of California San Diego, La Jolla, California, USA

<sup>3</sup>Global Modeling and Assimilation Office, NASA Goddard Space Flight Center, Greenbelt, Maryland, USA

<sup>4</sup>GESTAR-II, University of Maryland Baltimore County, Baltimore, Maryland, USA

<sup>5</sup>Center for Western Weather and Water Extremes, Scripps Institution of Oceanography, University of California San Diego, La Jolla, California, USA

<sup>6</sup>NSF NCAR Mesoscale and Microscale Meteorology Laboratory, Boulder, Colorado, USA

## **Contents of this file**

Text S1 to S3  
Figures S1 to S3

## **Introduction**

Within this supporting information we provide further explanation for specific characteristics of some ARO retrievals simulated with the forward model. Primarily, the occultations 2021.024.01.33.E36R and 2021.024.01.21.R02R presented in the main manuscript in Figs. 5 and 10, respectively, are discussed to support main conclusions. It is shown that a link between horizontal variability of the atmosphere and bending angle deviations can be established based on dropsonde observations in addition to ERA5 reanalysis fields employed in the simulations. Readers are referred to AR Recon data webpage ([https://cw3e.ucsd.edu/arrecon\\_data/](https://cw3e.ucsd.edu/arrecon_data/)) for more dropsonde profiles, amongst other observations.

### **Text S1.**

The dropsonde profiles at the east end of the northern G-IV transect show multiple upper level inversion layers, in particular one near 7.5 km that separates the air mass with the southwesterly jet stream from a higher moisture layer with southerly winds. This corresponds in height to the level of the sharp increase in the bending angle at 8.2 km impact height in the

ARO profile 2021.024.01.33.E36R discussed in the manuscript. This upper level inversion is an extensive feature present in the other profiles in the area.

**Text S2.**

Forward simulations with the tangent point drift are based on a series of cross-sections that are often characterized by distinct atmospheric properties. This is shown to affect bending angle departures for the occultation 2021.024.01.21.R02R for which the 2D bending angle is less than the 1D bending angle. Figure S2 shows locations of two representative cross-sections for this event where the ray-path would extend well into the dry region outside the IVT feature. Taking into account the 2D structure along the ray-path would lead to less bending therefore explaining bending angle differences of 5-10 % below 6 km impact height relative to 1D, particularly in the impact height range of 3.5-4.5 and 5-6 km.

**Text S3.**

The characteristics of IVT in the vicinity of occultation 2021.024.01.21.R02R can be further supported by examining the transect of dropsonde profiles for IOP04. The Skew-T diagrams also show that the profiles are drier in mid-levels to the northwest, especially for the extent of ERA5 cross-section outside the range of tangent point drift. The 2D slice gets more dry air within pressure levels of 700 to 400 hPa (4.5-7 km impact height) as well as from 850 to 700 hPa (3.5-4.5 impact height) that are shown to contribute to larger bending angles in 1D simulation.

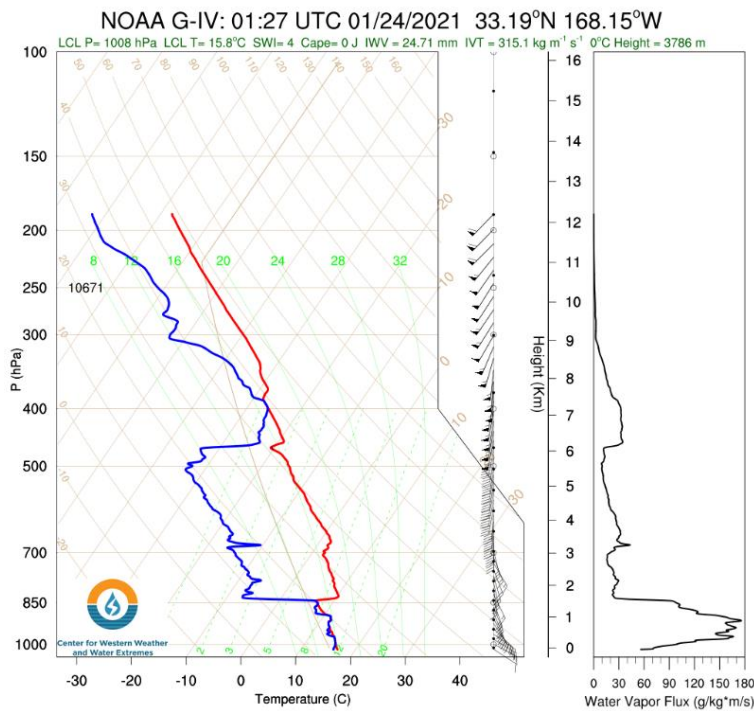


**Figure S1.** Skew-T diagram of dropsonde released at 01:27 UTC on 24 Jan 2021 in IOP04 near the location of the ARO profile 2021.024.01.33.E36R.

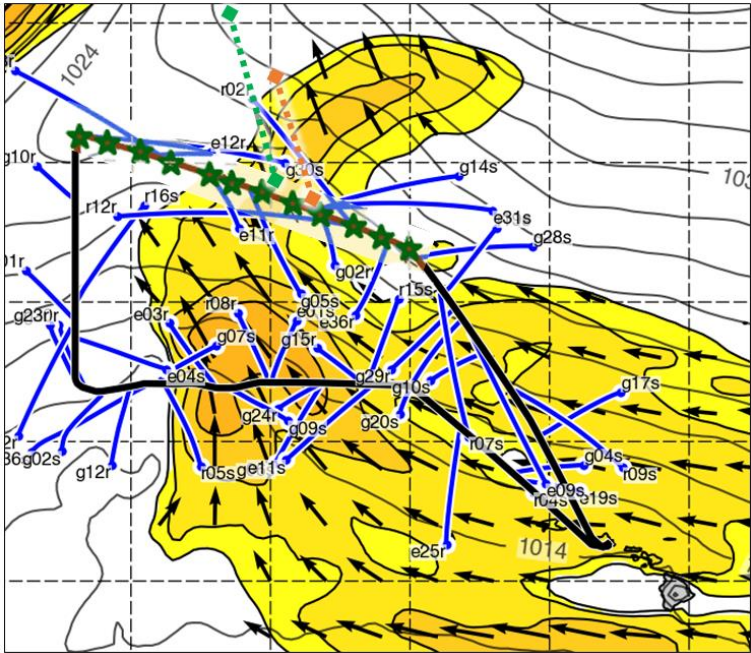


**Figure S2.** IOP04 flight track with locations of dropsondes (green stars) deployed along northern leg. Blue lines illustrate distributions of tangent points as they drift during ARO events. Additionally, the occultations are labeled with identifiers of GNSS occulting satellites, such as the rising occultation to GLONASS satellite R02. The orientation of occultation plane (azimuth to GNSS with respect to north) is marked with green and orange dotted lines representative for tangent point altitudes of 1.5 - 3.5 km and 3.5 - 6.5 km, respectively.

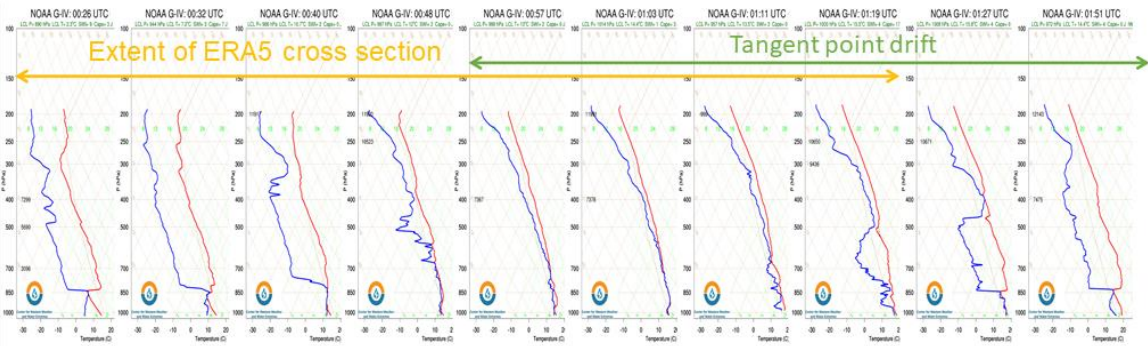


**Figure S3.** Transect of dropsonde profiles for IOP04 supporting ARO profile 2021.024.01.21.R02R observed at 37.2°N, 170.5°W. Green marks the extent of ARO observation as it drifts away from the reference tangent point which serves as the center for the cross-section through ERA5 field with the extent marked in orange.